

Ni^{2+} supported on hydroxyapatite-core-shell $\gamma\text{-Fe}_2\text{O}_3$ nanoparticles: a novel, highly efficient and reusable lewis acid catalyst for the regioselective azidolysis of epoxides in water

Sami Sajjadifar · Zahra Abbasi · Eshagh Rezaee Nezhad ·
Mojtaba Rahimi Moghaddam · Saaid Karimian ·
Sara Miri

Received: 4 February 2013 / Accepted: 20 June 2013 / Published online: 4 July 2013
© Iranian Chemical Society 2013

Abstract In this research, Ni^{2+} supported on hydroxyapatite-core-shell magnetic $\gamma\text{-Fe}_2\text{O}_3$ nanoparticles ($\gamma\text{-Fe}_2\text{O}_3\text{@HAp-Ni}^{2+}$) as a novel, efficient, reusable and heterogeneous catalyst was reported. In this protocol, we used this catalyst for the ring opening of epoxide with sodium azide in water. The catalyst can be readily isolated using an external magnet and no obvious loss of activity was observed when the catalyst was reused in seven consecutive runs. The mean size and the surface morphology of the nanoparticles were characterized by transmission electron microscopy, scanning electron microscope, vibrating sample magnetometry, X-ray powder diffraction and Fourier transform infrared techniques.

Keywords $\gamma\text{-Fe}_2\text{O}_3 \cdot \text{Ni}^{2+}$ supported · Lewis acid · Epoxide · Regioselective · Azidohydrins

Introduction

Recently, the application of nanoparticles (NPs) as attractive and interesting materials has been more and more increased, because of their high surface area and unique magnetic properties. Moreover, they have a wide range of usage in various fields; such as magnetic fluids [1], biology and medical applications [2], magnetic resonance imaging [3], data storage [4], environmental remediation [5], and their application as catalysts in organic transformations [6, 7].

Besides, the utilization of magnetic nanoparticles as heterogeneous and easily recycled catalysts has gained a significant attention. Moreover, they can be used in various organic reactions such as knoevenagel reaction [8, 9], nucleophilic substitution reactions of benzyl halides [10], epoxidation of alkenes [11], synthesis of α -amino nitriles [12], hydrogenation of alkynes [13], esterifications [14], CO_2 cycloaddition reactions [15], Suzuki coupling reactions [16] and three-component condensations [17].

2-Azidoalcohols would also be regarded as useful compounds in organic synthesis as either precursors of 2-amino alcohols or in the chemistry of carbohydrates, nucleosides, lactames, and oxazolines [18]. These compounds are versatile intermediates in organic synthesis and increasingly important in drugs and pharmaceuticals [19, 20]. The ring opening of epoxides, which have been innovation ways to obtain the direct azidolysis of epoxides in the presence of sodium azide, are frequently performed under several different conditions [21–25]. But some of these methods are limited to specific epoxides and are not applicable as versatile reagents in the preparation of azidohydrins; it is worth mentioning that these methods suffer from disadvantages such as long reaction times, low regioselectivity, using of expensive catalysts and difficulty in preparation of catalysts, difficulty in work-up and isolation of products. Therefore, it seems that there is still a need for development of novel methods that proceed under green and ecofriendly conditions.

In this work, $\gamma\text{-Fe}_2\text{O}_3\text{@HAp-Ni}^{2+}$ was synthesized and used as catalyst for the ring opening of epoxide with sodium azide in water. We thought that there is scope for further innovation towards milder reaction conditions, shorter reaction time, and high yields, which can be achieved using $\gamma\text{-Fe}_2\text{O}_3\text{@HAp-Ni}^{2+}$, as reaction media as well as a promoter in the absence of any toxic solvents.

S. Sajjadifar · Z. Abbasi · E. Rezaee Nezhad (✉) ·
M. R. Moghaddam · S. Karimian · S. Miri
Department of Chemistry, Payame Noor University,
PO BOX 19395-4697, Tehran, Iran
e-mail: e.rezaee66@yahoo.com

Experimental section

General

Products were characterized by comparison of their spectroscopic data (^1H NMR, ^{13}C NMR and IR) and physical properties with those reported in the literature. NMR spectra were recorded in DMSO- d_6 on a Bruker advanced DPX 500 and 400 MHz instrument spectrometers using TMS as internal standard. IR spectra were recorded on a Frontier Fourier transform infrared (FTIR) (Perkin Elmer) spectrometer using a KBr disk. All yields refer to isolated products. The characterization Ni^{2+} supported on hydroxyapatite-core-shell $\gamma\text{-Fe}_2\text{O}_3$ NPs, and its structural and morphological analysis was carried out by transmission electron microscopy (TEM), scanning electron microscope (SEM), vibrating sample magnetometry (VSM), X-ray diffractometer (XRD) and FTIR techniques. The phases present in the magnetic materials were analyzed using a powder XRD, Philips (Holland), model X' Pert with $\text{CuK}\alpha 1$ radiation ($\lambda = 1.5406 \text{ \AA}$), and the X-ray generator was operated at 40 kV and 30 mA. Diffraction patterns were collected from $2\theta = 20^\circ\text{--}80^\circ$.

Preparation of $\gamma\text{-Fe}_2\text{O}_3\text{@HAp-Ni}^{2+}$

In this study, $\gamma\text{-Fe}_2\text{O}_3\text{@HAp-Ni}^{2+}$ was prepared in two steps. The iron oxide magnetic particles (IOMP) were synthesized by chemical coprecipitation technique of ferric and ferrous chlorides in aqueous solution. Solutions of $\text{FeCl}_3\cdot 6\text{H}_2\text{O}$ (0.25 mol L^{-1}) and $\text{FeCl}_2\cdot 4\text{H}_2\text{O}$ (0.125 mol L^{-1}) were mixed and precipitated with NH_4OH solution (25 %) at pH 12, while stirring vigorously. The black suspension, which formed immediately, was maintained at 70°C for approximately 1 h and washed several times with ultra-pure water until the pH decreased to 7. IOMP/HAP was prepared by the impregnation method according to known procedures with some modifications [26]. Then hydroxyapatite-core-shell $\gamma\text{-Fe}_2\text{O}_3$ NPs (0.6 g) was introduced into 100 ml of distilled water containing

6.4 mmol of $\text{NiCl}_2\cdot 6\text{H}_2\text{O}$. The mixture was stirred (500 rpm) for 48 h, filtered, and washed several times with ethanol. The recovered solid was dried at 50°C overnight (Scheme 1). The mean size and the surface morphology of the Ni^{2+} supported on hydroxyapatite-core-shell $\gamma\text{-Fe}_2\text{O}_3$ -NPs were characterized by TEM, SEM, VSM, XRD and FTIR techniques.

Reactions of epoxides with NaN_3 catalyzed by $\gamma\text{-Fe}_2\text{O}_3\text{@HAp-Ni}^{2+}$

$\gamma\text{-Fe}_2\text{O}_3\text{@HAp-Ni}^{2+}$ (20 mg) was added to a mixture of the epoxide (1.0 mmol) and NaN_3 (3 mmol) in water (5 mL). The reaction mixture was magnetically stirred at 80°C for the appropriate time. Progress of reaction was monitored by TLC using ethylacetate:*n*-hexane (1:4). After reaction completion, the mixture was extracted with ethyl ether (5 mL \times 3), washed with brine, dried with CaCl_2 and evaporated under reduced pressure. The desired azido-hydrines were obtained in good to excellent isolated yields (84–93 %).

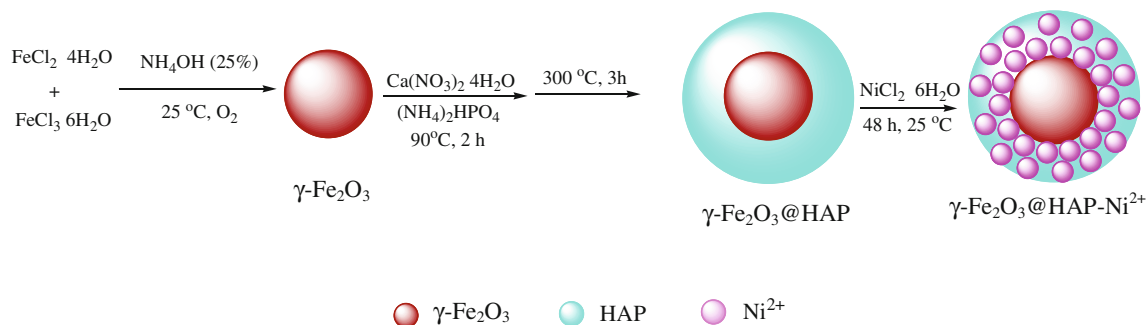
The catalyst can be separated from the reaction mixture using an external magnetic field; it was recovered with a simple magnet after the dilution of the reaction mixture with water.

The spectral data (^1H NMR, ^{13}C NMR and IR) of some representative compounds are given below:

Spectral data for 1-Azido-3-phenoxy-2-propanol (Entry 1). IR vmax/cm^{-1} : 2103(N_3) ^1H NMR (CDCl_3 , 400 MHz): 3.45–3.54 (m, 2H), 3.89 (m, 1H), 3.97–4.03 (m, 2H), 4.18 (s, 1H), 6.95–7.00 (m, 2H), 7.02–7.06 (m, 1H), 7.27–7.36 (m, 2H) ^{13}C NMR (CDCl_3 , 100 MHz): 53.51, 69.21, 69.30, 114.35, 121.16, 129.42, 158.36.

Spectral data for 2-Azido-2-phenyl-1-ethanol (Entry 2). IR vmax/cm^{-1} : 2102(N_3) ^1H NMR (CDCl_3 , 400 MHz): 3.37 (s, 1H), 3.74 (m, 2H), 4.65–4.69 (m, 1H), 7.34–7.44 (m, 5H) ^{13}C NMR (CDCl_3 , 100 MHz): 66.37, 68.03, 127.49, 128.46, 128.61, 136.47.

Spectral data for 1-Azido-3-butoxy-2-propanol (Entry 3). IR vmax/cm^{-1} : 2102(N_3) ^1H NMR (CDCl_3 , 400 MHz):



Scheme 1 Synthesis of Ni^{2+} supported on hydroxyapatite-core-shell $\gamma\text{-Fe}_2\text{O}_3$

0.87 (t, 3H), 1.31–1.35 (m, 2H), 1.50–1.53 (m, 2H), 3.14 (s, 1H), 3.30–3.32 (m, 2H), 3.39–3.44 (m, 4H), 3.87 (m, 1H)
 ^{13}C NMR (CDCl_3 , 100 MHz): 13.78, 19.16, 30.74, 53.52, 69.74, 70.59, 70.71.

Result and discussion

Synthesis of $\gamma\text{-Fe}_2\text{O}_3\text{@HAp-Ni}^{2+}$ and its structural and morphological analysis

Fourier transform infrared spectra were recorded on a FTIR spectrometer (Perkin Elmer) with a spectral resolution of 4 cm^{-1} in the wave number range of $450\text{--}4,000\text{ cm}^{-1}$. The samples and KBr were fully dried before the FTIR analysis to exclude the influence of water.

The magnetic properties were assessed with a VSM (RIKEN DENSHI Co. Ltd., Japan). The magnetic properties of the particles were evaluated in terms of saturation magnetization and coactivity.

Scanning electronic microscopy, the morphology of the surface of Ni^{2+} supported on hydroxyapatite-core-shell $\gamma\text{-Fe}_2\text{O}_3$ NPs was investigated using a scanning electronic microscope of XL30 type (Netherlands).

The synthesis of Ni^{2+} supported on hydroxyapatite-core-shell $\gamma\text{-Fe}_2\text{O}_3$ NPs was depicted in Scheme 1. Figure 1 shows the XRD for Ni^{2+} supported on hydroxyapatite-core-shell $\gamma\text{-Fe}_2\text{O}_3$ NPs. The characterization of Ni^{2+} supported on hydroxyapatite-core-shell $\gamma\text{-Fe}_2\text{O}_3$ NPs was further carried out by FTIR (Fig. 2). The band at $3,417\text{ cm}^{-1}$ was assigned to the stretching and bending modes of the OH groups in the hydroxyapatite structure. The bands at $1,042\text{ cm}^{-1}$ were attributed to the asymmetric and symmetric stretching vibration of the phosphate group (PO_4^{3-}), and the bending modes of Fe–O were observed at $604, 558\text{ cm}^{-1}$. In addition, the band at 875 cm^{-1} indicated that HPO_4^{2-} may also be present in the hydroxyapatite as an impurity.

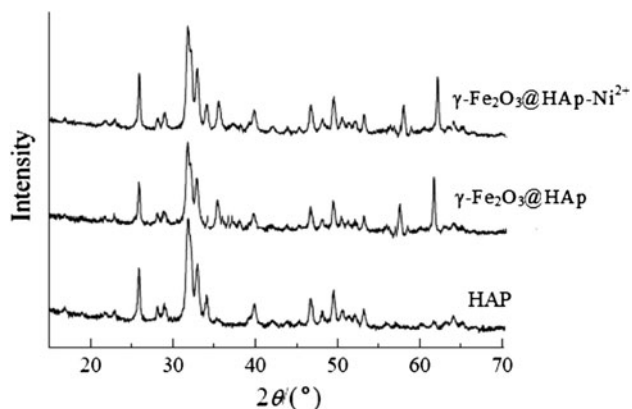


Fig. 1 XRD pattern of $\gamma\text{-Fe}_2\text{O}_3\text{@HAp-Ni}^{2+}$

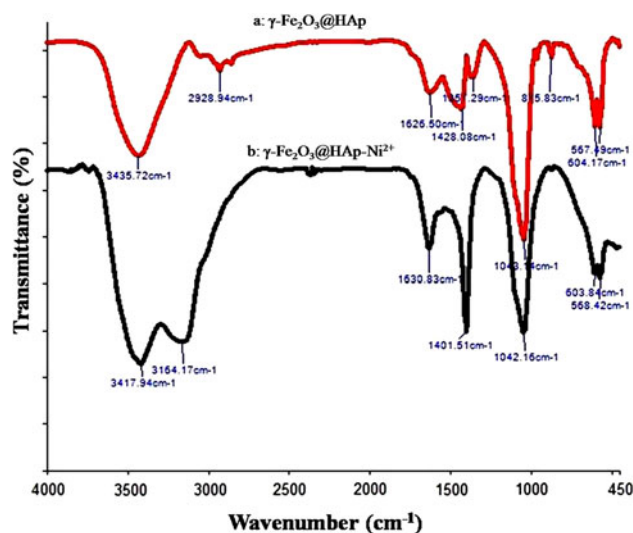


Fig. 2 FTIR spectra of a $\gamma\text{-Fe}_2\text{O}_3\text{@HAp}$, b $\gamma\text{-Fe}_2\text{O}_3\text{@HAp-Ni}^{2+}$

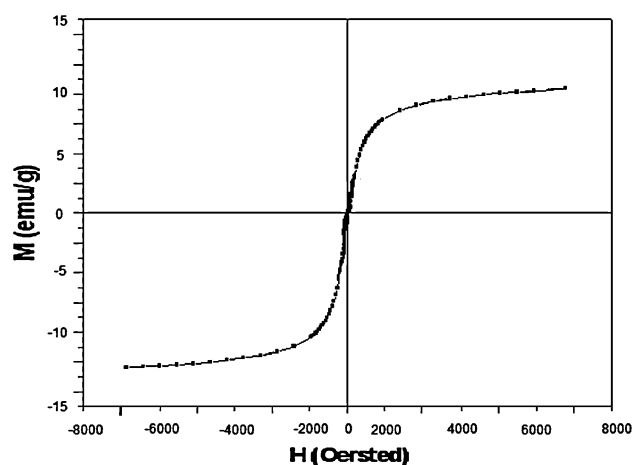


Fig. 3 Magnetization curves of $\gamma\text{-Fe}_2\text{O}_3\text{@HAp-Ni}^{2+}$

Figure 3 shows the magnetization curves for Ni^{2+} supported on hydroxyapatite-core-shell $\gamma\text{-Fe}_2\text{O}_3$ NPs. The magnetization curve gives a saturation magnetization value of 11.13 emu/g .

Scanning electronic microscopy image of Ni^{2+} supported on hydroxyapatite-core-shell $\gamma\text{-Fe}_2\text{O}_3$ NPs is given in Fig. 4.

Transmission electron micrographs provide more accurate information on the particle size, morphology and loading of Ni^{2+} supported on hydroxyapatite-core-shell $\gamma\text{-Fe}_2\text{O}_3$ NPs. These nanoparticles which consist of relatively small, nearly spherical particles, with an average size of 50 nm , are much smaller than the sizes obtained from the XRD measurements (Fig. 5).

Energy dispersive X-ray spectroscopy (EDX) was used for the morphological and microchemical analysis. The microchemical analysis was performed at 5 keV to

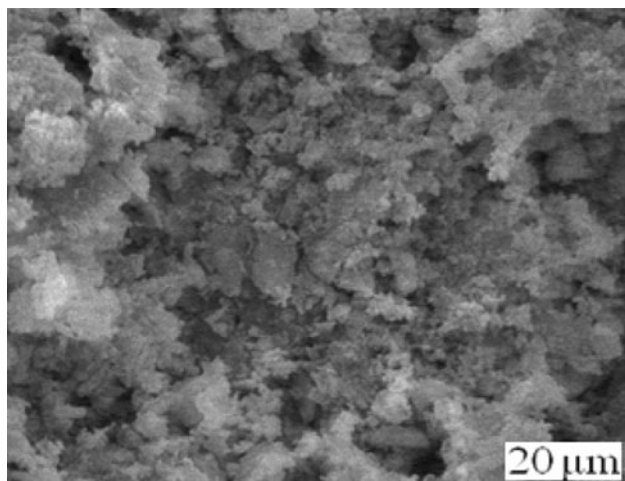


Fig. 4 SEM images of Ni²⁺/HAp- γ -Fe₂O₃ NPs

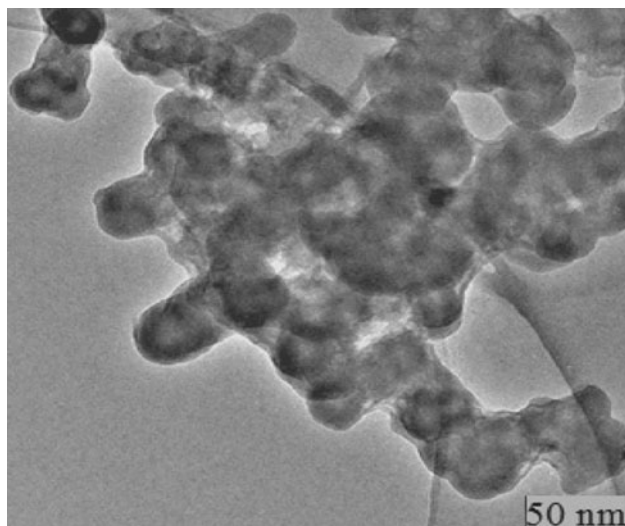


Fig. 5 TEM images of γ -Fe₂O₃@HAp-Ni²⁺

determine the chemical composition in the interior and at the surface of the particles. Particle size distributions for coated and uncoated IOMP were determined using a laser diffraction particle size analyzer (Cilas, 1064L).

Energy dispersive X-ray spectroscopy analyses were done to determine the chemical composition of the surface of the sample to support our observations on coating. EDX measurements were carried out on the same point with electrons having accelerating voltages of 20 and 5 keV, respectively. As 20 keV electrons have higher energy, they penetrate the sample deeper. On the other hand, with 5 keV electron there is a smaller penetration. Therefore, with 20 keV accelerating voltage it is likely to give the chemical composition of essentially the core of the particle. On the contrary with EDX studies with 5 keV, it may give the chemical composition essentially of the surface. Results of

EDX analysis of a typical sample, γ -Fe₂O₃@HAp-Ni²⁺, are given in Table 1.

We used atomic absorption spectroscopy for determination of Ni²⁺ loaded on catalyst; 240 mg of Ni²⁺ catalyst was found there.

Application of γ -Fe₂O₃@HAp-Ni²⁺ as magnetic catalyst for the regioselective azidolysis of epoxides in water

To evaluate the catalytic activity of γ -Fe₂O₃@HAp-Ni²⁺ catalyst in azidolysis of epoxides, the reaction of 2,3-epoxypropyl phenyl ether with sodium azide in water was examined to determine whether the use of γ -Fe₂O₃@HAp-Ni²⁺ was efficient and to investigate the optimized conditions (Table 2).

After optimizing the conditions, we examined the generality of these conditions to other substrates using several epoxides. Table 2 shows the results which clarifies that the reaction proceeds very efficiently in all cases. Different epoxides underwent ring opening easily in the presence of γ -Fe₂O₃@HAp-Ni²⁺ at 80 °C condition in water (Table 3). The products were formed in excellent yields. The conversion was complete in 20–40 min.

In view of the emerging importance of γ -Fe₂O₃@HAp-Ni²⁺ as novel reaction media, we wish to report the use of γ -Fe₂O₃@HAp-Ni²⁺ as efficient promoters for the ring opening of various epoxides. In this reaction, azidoalcohols

Table 1 EDX analysis of γ -Fe₂O₃@HAp-Ni²⁺

	Atomic weight% (5 keV)	Atomic weight% (20 keV)
O	21.04	30.98
P	23.83	14.32
Ca	55.12	26.13
Fe	–	23.74
Ni	–	4.82

Table 2 Optimization of experimental conditions for ring opening of epoxides

Entry	Catalyst (mg)	Temperature (°C)	Time (min)	Yield (%)
1	–	80	90	Trace
2	10	r.t.	90	Trace
3	10	60	90	38
4	10	80	90	52
5	15	80	60	67
6	20	80	20	90
7	25	80	20	86
8	20	100	20	90

Table 3 Ring opening of various epoxides in the presence of $\gamma\text{-Fe}_2\text{O}_3\text{@HAp-Ni}^{2+}$ in water

Entry	Substrate	Product(s)	Time (min)	Yield %
1			20	90
2			25	88 (11:89)
3			25	89
4			30	90
5			30	85
6			25	93
7			35	92
8			35	87
9			30	90
10			40	84

as products were obtained in good yields, short reaction times and avoid use of organic solvents (handling, cost, safety, pollution). Water is a desirable solvent for chemical reactions for reasons of cost, safety and environmental concerns; use of water in this reaction gave only greater regioselectivity ring opening of epoxide.

As it can be seen in Table 3, $\gamma\text{-Fe}_2\text{O}_3\text{@HAp-Ni}^{2+}$ as a catalyst was afforded good results in comparison to the other catalysts. In order to evaluate the efficiency of our introduced method, more recently developed methods were compared with our present method on the basis of the

yields and reaction times parameters. The results are given in Table 4.

Catalyst reusability is of major importance in heterogeneous catalysis. The recovery and reusability of the catalyst was studied using 2,3-epoxypropyl phenyl ether with sodium azide as model reaction. Since the catalyst can be separated from the reaction mixture using an external magnetic field, it was recovered with a simple magnet after the dilution of the reaction mixture with water. The catalyst was consecutively reused seven times without any noticeable loss of its catalytic activity (Table 5).

Table 4 Comparison of catalytic ability of catalysts

Entry	Catalyst/solvent/ temperature	Reaction time (h)	Yield %	References
1	Network polymer/water/ 80 °C	1.5	89	[21]
2	SiO ₂ -OPEG(300)/water/ reflux	2	89	[23]
3	[bmim]PF ₆ ([bmim]BF ₄)/ water/65 °C	3 (5)	95 (89)	[25]
4	β-Cyclodextrin/water/r.t.	5	45	[27]
5	AMP/Acetonitrile/r.t.	5	96	[28]
6	Polymeric PTC/water/r.t.	12	94	[29]
7	γ-Fe ₂ O ₃ @HAp-Ni ²⁺ / water/80 °C	20 min	90	This work

AMP ammonium-12-molybdophosphate, polymeric PTC poly[N-(2-aminoethyl)acrylamido]-trimethyl ammonium iodide

Table 5 The catalytic activity of γ-Fe₂O₃@HAp-Ni²⁺ in seven cycles

Run	1	2	3	4	5	6	7
Yield (%)	90	90	88	86	87	85	85

Conclusion

In this research, Ni²⁺ supported on hydroxyapatite-core-shell magnetic γ-Fe₂O₃ nanoparticles was readily synthesized and functionalized with Ni²⁺. We described a simple and highly efficient protocol for the regioselective azidolysis of epoxides. The advantages of the present procedure are its simplicity of operation, very short reaction times in comparison to the other procedures, and the high yields of products. In this way, the catalyst can be easily recovered by simple magnetic decantation and reused several times with no loss of activity.

Acknowledgments The authors gratefully acknowledge partial support of this work by Ilam Payame Noor University, Islamic Republic of Iran.

References

1. S. Chikazumi, S. Taketomi, M. Ukita, M. Mizukami, H. Miyajima, M. Setogawa, Y. Kurihara, J. Magn. Magn. Mater. **65**, 245–251 (1987)

2. A.K. Gupta, M. Gupta, Biomaterials **26**, 3995–4021 (2005)
3. S.I. Park, J.H. Kim, J.H. Lim, C.O. Kim, Curr. Appl. Phys. **8**, 706–709 (2008)
4. T. Hyeon, Chem. Commun. 927–934 (2003)
5. A. Lu, W. Schmidt, N. Matoussevitch, H. Bönemann, B. Spliethoff, B. Tesche, E. Bill, W. Kiefer, F. Schüth, Angew. Chem. **116**, 4403–4406 (2004)
6. S.C. Tsang, V. Caps, I. Paraskevas, D. Chadwick, D. Thompsett, Angew. Chem. **116**, 5763–5766 (2004)
7. Y. Polshettiwar, R.S. Varma, Green Chem. **12**, 743–754 (2010)
8. E. Karaoğlu, A. Baykal, M. Senel, H. Sözeri, M.S. Toprak, Mater. Res. Bull. **47**, 2480–2486 (2012)
9. Y. Zhang, C. Xia, Appl. Catal. A: General **366**, 141–147 (2009)
10. A.R. Kiasat, S. Nazari, J. Mol. Catal. A: Chem. **365**, 80–86 (2012)
11. M. Kooti, M. Afshari, Mater. Res. Bull. **47**, 3473–3478 (2012)
12. M.Z. Kassaee, H. Masrouri, F. Movahedi, Appl. Catal. A: General **395**, 28–33 (2011)
13. R. Abu-Reziq, D. Wang, M. Post, H. Alper, Adv. Synth. Catal. **349**, 2145–2150 (2007)
14. Y.Y. Jiang, C. Guo, H.S. Xia, I. Mahmood, C.Z. Liu, H.Z. Liu, J. Mol. Catal. B Enzym. **58**, 103–109 (2009)
15. X.X. Zheng, S.Z. Luo, L. Zhang, J.P. Cheng, Green Chem. **11**, 455–458 (2009)
16. A. Taber, J.B. Kirn, J.Y. Jung, W.S. Ahn, M.J. Jin, Synlett **15**, 2477–2482 (2009)
17. Q. Zhang, H. Su, J. Luo, Y.Y. Wei, Green Chem. **14**, 201–208 (2012)
18. S.W. Chen, S.S. Thakur, W. Li, C.K. Shin, R.B. Kawthekar, G.J. Kim, J. Mol. Catal. **259**, 116–120 (2006)
19. J.S. Yadav, B.V.S. Reddy, A.K. Basak, A.V. Narsaiah, Tetrahedron Lett. **44**, 1047–1050 (2003)
20. B.T. Smith, V. Gracias, J. Aube, J. Org. Chem. **65**, 3771–3774 (2000)
21. A. Mouradzadegun, A.R. Kiasat, P. Kazemian Fard, Catal. Commun. **29**, 1–5 (2012)
22. F. Heidarzadeh, A. Zarei, J. Chem. Soc. Pak. **34**, 593–598 (2012)
23. A.R. Kiasat, M. Zayadi, Catal. Commun. **9**, 2063–2067 (2008)
24. F. Kazemi, A.R. Kiasat, S. Ebrahimi, Synth. Commun. **33**, 999–1004 (2003)
25. J.S. Yadav, B.V. Reddy, B. Jyothirmay, M.S.R. Murty, Tetrahedron Lett. **46**, 6559–6562 (2005)
26. K. Donadel, D.V. Marcosand, C.M. Mauro, An. Acad. Bras. Ciêns. **81**, 179–186 (2009)
27. A. Kamal, M. Arifuddin, M.V. Rao, Tetrahedron Asymmetry **10**, 4261–4264 (1999)
28. B. Das, V.S. Reddy, M. Krishnaiah, Y.K. Rao, J. Mol. Catal. A: Chem. **270** 89–92 (2007)
29. B. Tamami, H. Mahdavi, Tetrahedron Lett. **42**, 8721–8724 (2001)